Crystal structure of the IL-2 signaling complex: Paradigm for a heterotrimeric cytokine receptor

Deborah J. Stauber*[†][‡], Erik W. Debler*[†], Patricia A. Horton*[‡], Kendall A. Smith[§], and Ian A. Wilson*[¶]

*Department of Molecular Biology and The Skaggs Institute for Chemical Biology, The Scripps Research Institute, 10550 North Torrey Pines Road, La Jolla, CA 92037; and [§]Division of Immunology, Department of Medicine, Weill Medical College of Cornell University, New York, NY 10021

IL-2 is a cytokine that functions as a growth factor and central regulator in the immune system and mediates its effects through ligand-induced hetero-trimerization of the receptor subunits IL-2Rα, IL-2Rβ, and γ$_c$. Here, we describe the crystal structure of the trimeric assembly of the human IL-2 receptor ectodomains in complex with IL-2 at 3.0 Å resolution. The quaternary structure is consistent with a stepwise assembly from IL-2/IL-2Rα to IL-2/IL-2Rα/IL-2Rβ to IL-2/IL-2Rα/IL-2Rβ/γ$_c$. The IL-2Rα subunit forms the largest of the three IL-2/IL-2R interfaces, which, together with the high abundance of charge–charge interactions, correlates well with the rapid association rate and high-affinity interaction of IL-2Rα with IL-2 at the cell surface. Surprisingly, IL-2Rα makes no contacts with IL-2Rβ or γ$_c$, and only minor changes are observed in the IL-2 structure in response to receptor binding. These findings support the principal role of IL-2Rα to deliver IL-2 to the signaling complex and act as regulator of signal transduction. Cooperativity in assembly of the final quaternary complex is easily explained by the extraordinarily extensive set of interfaces found within the fully assembled IL-2 signaling complex, which nearly span the entire length of the IL-2Rβ and γ$_c$ subunits. Helix A of IL-2 wedges tightly between IL-2Rβ and γ$_c$ to form a three-way junction that coalesces into a composite binding site for the final γ$_c$ recruitment. The IL-2/γ$_c$ interface itself exhibits the smallest buried surface and the fewest hydrogen bonds in the complex, which is consistent with its promiscuous use in other cytokine receptor complexes.

common γ chain | cooperativity | IL-2 receptor | receptor assembly | structure–activity relationship

In 1976, lymphocyte-conditioned medium was found to support the long-term growth of T lymphocytes (T cells) (1), but the active component was not characterized as a variably glycosylated 15.5-kDa protein until 1981 (2). Subsequently, IL-2 was purified to homogeneity (3), and its cDNA was cloned in 1983 (4). The discovery of IL-2 permitted the creation of monoclonal T cells (5), which were instrumental in the characterization of many aspects of T cell biology. IL-2 is the primary cytokine responsible for the rapid expansion, differentiation, and survival of antigen-selected T cell clones during an immune response, but is also important for B cell, natural killer (NK) cell (6), and regulatory T cell (T$_{reg}$) (7) function.

IL-2 was the first cytokine found to mediate its effects via a cell surface binding site with all of the characteristics of classic hormone receptors, including high affinity, stereospecificity, and saturability (8). Kinetic binding studies revealed that the high affinity binding ($K_d \approx 10$ pM) to the IL-2 receptor (IL-2R) is due to a rapid rate of association ($k_{on} \approx 10^7$ M^{-1}·s^{-1}), but relatively slow dissociation rate ($k_{off} \approx 10^{-4}$ s^{-1}) (9). The high-affinity IL-2R comprises three separate, noncovalently linked chains, termed α (IL-2Rα, p55, CD25) (10), β (IL-2Rβ, p75, CD122) (11, 12), and γ (γ$_c$, IL-2Rγ, p65, CD132) (13), the latter being a common receptor component for many cytokines, including IL-4, IL-7, IL-9, IL-15, and IL-2 (14). IL-2Rα contributes the rapid association rate of IL-2 binding, whereas IL-2Rβ is responsible for its slow dissociation rate (9).

A critical number of IL-2Rs must be triggered before an individual T cell will make the irrevocable, quantal (all-or-none) decision to pass through the G$_1$ restriction point so as to undergo DNA replication and subsequent mitosis (15, 16). However, exactly how the cell senses this threshold of triggered IL-2Rs has remained obscure. A clue to this issue may then reside in the structure–activity relationship (SAR) of the IL-2/IL-2R interaction.

Here, we present the crystal structure of the fully assembled, human IL-2 receptor ectodomains in complex with its ligand at 3.0 Å resolution. The molecular architecture of this heterotrimeric receptor can now be analyzed to decipher the assembly, signaling, and disassembly mechanisms of this enigmatic cytokine receptor complex, and provide insights into the cooperativity of high-affinity binding, as well as the promiscuous use of γ$_c$ in other cytokine receptor complexes.

Results

Assembly of the Quaternary IL-2 Signaling Complex. The high-affinity complex of IL-2 with its extracellular IL-2Rα, IL-2Rβ, and γ$_c$ receptor domains was assembled from the individual receptor ectodomains expressed in insect cells. Throughout purification of γ$_c$, this receptor subunit existed as a stable homotrimer, as determined by gel filtration. When incubated at 37°C in the presence of IL-2Rα, IL-2Rβ, and IL-2, the γ$_c$ trimer could dissociate and incorporate into the stable quaternary IL-2 signaling complex. However, upon chemical deglycosylation, γ$_c$ aggregated and could not be dissociated for engagement in the high-affinity complex. Thus, self interaction through trimerization and surface carbohydrate sites on γ$_c$ may serve an important solubility role, masking epitopes for IL-2 and IL-2Rβ recognition until formation of a productive signaling complex.

Structure Determination of the Quaternary IL-2 Signaling Complex. The 3.0-Å crystal structure was determined by molecular replacement by using the coordinates from an independently assembled IL-2/IL-2R complex (17), in which mutations at Asn-17[β]Gln and Asn-45[β]Gln eliminated two glycosylation sites and which crystallized in a different space group (C2). A brief comparison of the IL-2/IL-2R complexes in the triclinic (here) and the monoclinic crystal form (17) is presented in *Supporting Materials and Methods*, which is published as supporting information on the PNAS web site. The x-ray structure was refined to R_{free} and R_{cryst} of 26% and 22%, respectively (Table 2, which is published as supporting information on the PNAS web site). Two independent complexes in the asymmetric unit offered a valu-

Table 1. Properties of the IL-2/IL-2Rα/IL-2Rβ/γc interfaces

	IL-2	IL-2Rα	IL-2Rβ	γc (adjacent molecule)
IL-2Rα				
Total buried surface area, Å²	1590/1690			1150/1100
% main chain buried surface area	20/22			17/17
% polar buried surface area	67/68			67/63
No. van der Waals contacts	94/91			70/80
No. hydrogen bonds	6/6			9/9
Shape correlation (S_c)	0.71/0.64			0.68/0.78
Affinity constant (K_d), from ref. 28	10 nM			ND
IL-2Rβ				
Total buried surface area, Å²	1160/1150	0		
% main chain buried surface area	12/12	0		
% polar buried surface area	69/70	0		
No. van der Waals contacts	67/76	0		
No. hydrogen bonds	10/10	0		
Shape correlation (S_c)	0.68/0.74	0		
Affinity constant (K_d), from ref. 28	144 nM	278 nM		
γc				
Total buried surface area, Å²	970/980	0	1640/1610	
% main chain buried surface area	18/16	0	17/14	
% polar buried surface area	86/63	0	74/74	
No. van der Waals contacts	2/2	0	97/90	
No. hydrogen bonds	71/74	0	14/14	
Shape correlation (S_c)	0.76/0.72	0	0.64/0.63	
Affinity constant (K_d), from ref. 28	ND*	ND	ND	

ND, not detected.

*However, weak binding ($K_d > 50$ μm) was detected in other assays, e.g. ref. 40.

able cross validation of key architectural features of the signaling complex (Table 1). In the following analyses, however, only values pertaining to the first complex (chain IDs A, B, C, and D under PDB ID code 2ERJ) are cited unless structural differences are explicitly highlighted or the values differ significantly.

Architecture of the Quaternary IL-2 Receptor Signaling Complex. The assembly of the IL-2Rβ and γc ectodomains bound to IL-2

recapitulate architectural features of the prototypic, human growth hormone (GH) receptor dimer in that a four-helix bundle cytokine is clamped between the elbow regions of two receptor subunits that are roughly related by pseudo-2-fold symmetry, but with a slight translation of γc relative to IL-2Rβ (Fig. 1) (18). The interdomain region of γc contacts IL-2 helices A and D (classical binding site I), and the elbow region of IL-2Rβ contacts IL-2 helices A and C (classical binding site II) (18). IL-2Rα interacts

Fig. 1. Architecture of the human IL-2R signaling complex. Shown are side (*A*) and top (*B*) views of the quaternary IL-2 signaling assembly. IL-2 binds to the elbow regions of IL-2Rβ and γc. IL-2Rα docks on top of this assembly without forming any contacts with the other two receptor subunits. Six N-linked carbohydrates (S1 to S6) are displayed as ball-and-stick models. S1 is wedged between D1 and D2 of IL-2Rβ and, thus, contributes to the stabilization of a specific D1/D2 interdomain angle.
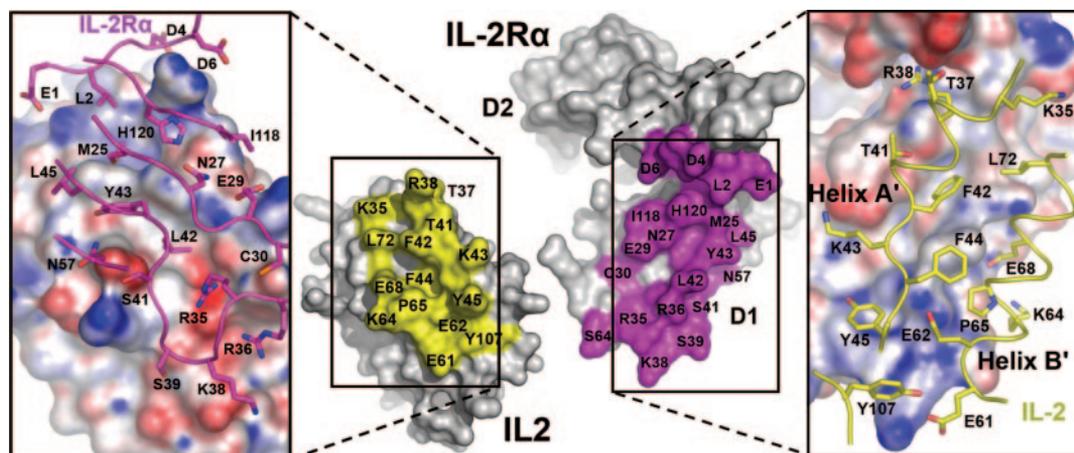
IMMUNOLOGY

Fig. 2. Interface between IL-2Rα and IL-2. Open-book representation of the IL-2/IL-2Rα interface. The electrostatic potential was mapped onto the molecular surface and contoured at ±35kT/eV (blue/red). The interface features a hydrophobic center, flanked by a large number of salt bridges and other polar contacts. The strong electrostatic component of this interaction serves to rapidly capture IL-2 and, thus, to dominate the k_{on} rate of IL-2 binding to the IL-2R.

mainly with the long connection between helices A and B that include helices A′ and B′ of IL-2, in a region recently termed "site IV" (19). IL-2Rα surprisingly does not contact IL-2Rβ or γc, and the three interaction sites on IL-2 generally do not overlap with each other, except for a small, but significant, region (see below). The IL-2 molecule in this quaternary complex undergoes only minimal conformational changes, the most significant of which is the ordering of the BC loop (residues 74–81) due to crystal-packing interactions. The IL-2Rβ and γc constructs terminate just 6 and 7 residues from the transmembrane domains, respectively (20). Thus, we can estimate the distance from the observed C terminus (Gly-165$^\alpha$) of IL-2Rα to the membrane to be ≈40 Å, consistent with the predicted unstructured 54-residue linker between Gly-165$^\alpha$ and the putative transmembrane domain (20).

Structure of IL-2Rα and Its Interface with IL-2. IL-2Rα folds into two "sushi-like" domains D1 and D2, which form five-stranded β-sheet sandwiches. These domains are disposed at ≈75° to each other, as in the crystal structure of IL-2Rα complexed with IL-2 (19). D1 accounts for the majority (82%) of the total buried surface area (1,590 Å^2) between IL-2Rα and IL-2, whereas D2 contributes only to a minor extent. The nature of the IL-2/IL-2Rα interface reveals a striking dichotomy of a hydrophobic center dominated by IL-2Rα residues Leu-2$^\alpha$, Met-25$^\alpha$, Leu-42$^\alpha$, and Tyr-43$^\alpha$ and IL-2 residues Phe-42^{IL-2}, Phe-44^{IL-2}, Tyr-45^{IL-2}, Pro-65^{IL-2}, and Leu-72^{IL-2}, and a polar periphery featuring five ion pairs (Lys-38$^\alpha$/Glu-61^{IL-2}, Arg-36$^\alpha$/Glu-62^{IL-2}, Glu-1$^\alpha$/Lys-35^{IL-2}, Asp-6$^\alpha$/Arg-38^{IL-2}, and Glu-29$^\alpha$/Lys-43^{IL-2}; Fig. 2). Seven hydrogen bonds are formed between IL-2 and IL-2Rα (Table 3, which is published as supporting information on the PNAS web site). No significant differences in side- and main-chain conformations are observed at the core of the IL-2/IL-2Rα interface, but some variation in total buried surface area and shape correlation S_c in the two complexes (0.71 and 0.64, by using a 1.7-Å probe) is noted (Table 1). A slight rigid-body rotation (10°) of IL-2Rα with respect to IL-2 seems to result from different crystal packing environments that would give rise to the slight variations in shape complementarity and buried surface.

Architecture of IL-2Rβ and γc. The ectodomains of IL-2Rβ and γc possess a cytokine-binding homology region, which is divided in two fibronectin type-III (FN-III) domains termed D1 and D2. Each domain contains seven β-strands that form a sandwich of two antiparallel β-sheets. The N-terminal D1 domains of IL-2Rβ

and γc both conform to the hybrid type of the Ig fold (21) where the C′ strand hydrogen bonds with both faces of the β-sandwich (Fig. 1), similar to erythropoietin receptor (EPOR) (22). In contrast, the D2 domains belong to the switched type of Ig folds, where strand C′ hydrogen bonds only with strand C. Domain D1 (residues 6–99) and D2 (103–209) of IL-2Rβ are disposed at an elbow angle of 73°, characteristic of class I cytokine receptors (GHR, 64°; IL-4R, 82°; EPOR, 62° and 77°), whereas in γc the elbow angles between D1 (32–125) and D2 (129–226) increases to 92° and 98°, respectively, more typical of class II cytokine receptors (IL-10R1, 93°; IFN-αR2, 100°; tissue factor, 118°) (23). The distinct elbow angle in γc is also accompanied by a more extended interdomain region. Finally, the D1 and D2 linker regions of IL-2Rβ (residues 100–102) and γc (126–128) both adopt a 3_{10} helical conformation.

A common feature of class I cytokine receptor domains includes two highly conserved disulfide bridges in D1 that link strands A to B, and strands C′ to E, as in IL-2Rβ and γc. IL-2Rβ D1 contains an additional disulfide between strands C and F (Cys-33$^\beta$-Cys-84$^\beta$). D2 of γc exhibits another unique disulfide that connects loops BC2 and FG2 (Cys-160$^\gamma$-Cys-209$^\gamma$) and significantly contributes to the interface with IL-2 (Fig. 4). In D2 of both IL-2Rβ and γc, a tryptophan-arginine ladder on sheet C′-C-F-G, that contains the highly conserved WSXWS motif, is present, as in other cytokine receptors (18, 24).

In IL-2Rβ, a particularly well defined glycan structure, consisting of four sugars N-linked to Asn-17, is wedged between D1 and D2 (Fig. 1A and Fig. 6, which is published as supporting information on the PNAS web site). The α1,6-linked core fucose forms four hydrogen bonds with Arg-105$^\beta$ and Leu-106$^\beta$ of D2. Moreover, the four sugars make numerous van der Waals contacts with D1 and D2, which may help stabilize a precise orientation of the respective fibronectin type-III domains to each other.

Interface Between IL-2Rβ and IL-2. IL-2 forms the second largest interface with IL-2Rβ (1,150 Å^2, Table 1) with good shape complementarity (0.68) and high specificity via 10 hydrogen bonds (Table 3). Recognition of IL-2 by IL-2Rβ is dominated by the central, protruding Tyr-134$^\beta$, which contributes 17% of the buried surface area on IL-2Rβ (Fig. 3). For IL-2, Asp-20^{IL2} and His-16^{IL2} seem to be the most critical residues; Asp-20^{IL2} hydrogen bonds to His-133$^\beta$ and Tyr-134$^\beta$, whereas His-16^{IL2} is tucked into a slot created by Tyr-134$^\beta$, Gln-188$^\beta$, and the methyl groups of Thr-74$^\beta$ and Thr-73$^\beta$. Major van der Waals contacts in

Fig. 3. Interface of IL-2Rβ with IL-2 and γ$_c$. The interface of IL-2Rβ (cyan/red) and IL-2 (yellow/red) is intermediate in buried surface area among the three IL-2/IL-2R interfaces. Asp-20 and His-16 of IL-2 are located at the center of the binding region and are involved in many van der Waals contacts and hydrogen bonds. The interface features the highest number of hydrogen bonds, consistent with its high specificity and low k_{off} rate of IL-2 dissociation. The large contact area with γ$_c$ is colored brown and includes two residues (red) that also interact with IL-2 (red residues).

the interface are also made with Arg-41[β], Val-75[β], His-133[β], Leu-19[IL2], Asp-84[IL2], Asn-88[IL2], and Val-91[IL2].

Interface Between γ$_c$ and IL-2. The γ$_c$/IL-2 interaction (970 Å^2) is the smallest of the three IL-2/IL-2R interfaces, although with good surface complementarity (0.72). Furthermore, this contact surface features only two hydrogen bonds (Table 3) and weak electrostatic interactions (Fig. 4), indicating low specificity. The contribution of main-chain atoms to the buried surface area is intermediate (17% on average) between those of IL-2Rα (21%) and IL-2Rβ (12%) (Table 1). Tyr-103[γ], His-159[γ], and Leu-208[γ] together with the disulfide (Cys-160[γ]-Cys-209[γ]) contribute 53% of the buried surface on γ$_c$ and represent the major binding determinant. The importance of the disulfide bridge was previously appreciated from mutagenesis data (25, 26), but its direct involvement in ligand binding was unexpected. With a buried surface area of 72 Å^2 and one hydrogen bond, Gln-126[IL2] is the most critical IL-2 residue that contacts γ$_c$ in accordance with biochemical data (27). Glu-15[IL2], Thr-123[IL2], and Ile-129[IL2] contribute other significant interactions to the IL-2/γ$_c$ interface.

Interface Between IL-2Rβ and γ$_c$. In stark contrast to the relatively small IL-2/γ$_c$ interface, the IL-2R structure reveals a surprisingly large and specific interaction between the D2 receptor domains of IL-2Rβ and γ$_c$ (1,640 Å^2). The predominantly polar contacts are evenly distributed among the 22 residues of IL-2Rβ and 31 residues of γ$_c$ without any obvious hot-spot residues. The low percentage of aromatic residues among the side-chain contributions (12%), in combination with 14 hydrogen bonds, seems to enforce much higher specificity of γ$_c$ with IL-2Rβ than of γ$_c$ to IL-2. Glu-136[β] and

Fig. 4. Interface of γ$_c$ with IL-2 and IL-2Rβ. This γ$_c$ interface (green/red) with IL-2 (yellow/red) is characterized by the smallest total buried surface area and formation of only two hydrogen bonds. Strikingly, the elbow region of γ$_c$ engages only partially with IL-2. Furthermore, γ$_c$ exhibits a large elbow angle, which is atypical of class-I cytokine receptors. These structural properties are likely to contribute to promiscuity of this receptor subunit. The large contact area with IL-2Rβ is colored brown and includes three residues (red) which also interact with IL-2 (red residues).

His-138[β] form the hinge of the D1/D2 IL-2Rβ elbow and significantly interact with both IL-2 and γ$_c$. Similarly, Tyr-182[γ], Pro-207[γ], and Leu-208[γ] form the hinge of the D1/D2 γ$_c$ elbow and interact with both IL-2 and IL-2Rβ.

Interface Between IL-2Rα and γ$_c$: Crystal Artifact or Physiologically Relevant. A crystal contact of considerable size and specificity is formed between γ$_c$ and a symmetry-related IL-2Rα molecule in the neighboring unit cell. Remarkably, this interaction is observed in both copies of the asymmetric unit, as well as in another crystal form (17). IL-2Rα D2 strands H, I, and J interact with the surface of the γ$_c$ elbow region that is not involved in IL-2 binding. Structural features include high shape complementarity (0.68 and 0.78, respectively), a large buried surface area (1,150 Å^2) and nine interdomain hydrogen bonds. In this arrangement, the D2 domains of IL-2Rβ/γ$_c$ are parallel to each other, with their C termini toward the membrane (Fig. 7, which is published as supporting information on the PNAS web site). Such lateral interactions would lead to one-dimensional lattices of IL-2R complexes on the cell surface that could promote higher-order signaling assemblies, although no measurable affinity between soluble IL-2Rα and γ$_c$ has been detected (28). However, this same set of experiments also did not detect any binding between IL-2Rβ and γ$_c$, which in fact form an extensive interface in the fully assembled IL-2R.

Discussion

Despite only 10–20% sequence identity to other cytokine receptors, the IL-2Rβ and γ$_c$ ectodomains of the IL-2 receptor

IMMUNOLOGY

have long been recognized to consist of two tandem fibronectin type-III domains that contain sequence signature motifs as in other cytokine receptors (13, 29). As expected, a DALI search (30) identified other cytokine receptors, such as IL-4R (Z-score of 17.3, rms deviation (rmsd) of 2.4 Å over 176 residues) and erythropoietin receptor (16.5, 3.4 Å over 182 residues) as the closest structural homologs of IL-2Rβ and γ_c. However, the crystal structure of the complete IL-2/IL-2R complex now enables analysis of the organization of the quaternary assembly and the nature and extent of each of the IL-2/IL-2R interfaces and receptor subunit interactions, as well as the role of the individual receptor subunits in the high-affinity complex assembly and signal transduction.

The precise role of IL-2Rα has so far remained elusive. This receptor subunit, together with IL-2Rβ, can form a pseudo-high-affinity site for IL-2 on the cell surface ($K_d \approx 300$ pM), yet IL-2Rβ itself binds IL-2 only with modest affinity ($K_d \approx 450$ nM) (31). In contrast, a soluble form of IL-2Rβ comprising solely its ectodomain exhibits comparable IL-2 affinity ($K_d \approx 144$ nM) to its membrane-bound form, but only $\approx$2-fold increased affinity ($K_d \approx 64$ nM) upon addition of soluble IL-2Rα (28). Minor changes observed in the IL-2 structure in response to IL-2Rα binding are probably sufficient to explain the 2-fold increase in IL-2Rβ affinity for IL-2 in solution. However, because IL-2Rα does not make any interactions with IL-2Rβ, the massive difference in the K_d of IL-2 with membrane-anchored IL-2Rβ in the presence or absence of IL-2Rα suggests that this subunit primarily serves as a ligand carrier. For potent cell signaling, secreted IL-2 must be captured at the cell surface to minimize its loss by diffusion away from the cell. The high affinity of IL-2Rα for IL-2 and the large excess of IL-2Rα over IL-2Rβ and IL-2Rγ on activated T cells facilitate this capture and delivery to IL-2Rβ or to any IL-2Rβ/γ_c complex through two-dimensional cell surface diffusion. Computational modeling suggests that a stepwise assembly mechanism leads to a greater number of high-affinity signaling complexes than signaling via a preformed, fully assembled IL-2R, considering the thermodynamics, kinetics, receptor density, and cell density of the IL-2/T cell system (32). Alternatively, cooperativity in formation of the ternary IL-2/IL-2Rα/IL-2Rβ complex may result from a preformed IL-2Rα/IL-2Rβ complex on the cell surface, which would then undergo large-scale conformational rearrangements upon assembly to higher-order IL-2 signaling complexes. Isothermal titration calorimetry (ITC) experiments (28) have, in fact, measured significant affinity for this heterodimer ($K_d \approx 280$ nM), but the structure of the quaternary IL-2 complex is difficult to reconcile with this finding.

The preponderance of charge–charge interactions at the IL-2/IL-2Rα interface may serve to dominate the kinetics of IL-2 recruitment by its receptor. Long-range electrostatic interactions are known to accelerate the association rate k_{on}, whereas short range interactions govern the dissociation rate k_{off} (33). The rapid rate of IL-2 association with IL-2Rα (9) is then consistent with strong electrostatic interactions and high electrostatic complementarity, whereas the slow dissociation rate ascribed to IL-2Rβ (9) correlates well with the properties of the IL-2/IL-2Rβ interface (Table 1).

Thus, the IL-2Rα/IL-2 complex is likely to be preferentially delivered to IL-2Rβ, forming the pseudo-high-affinity complex, in agreement with isothermal titration calorimetry experiments (28). This complex then recruits γ_c, possibly from γ_c trimers, burying a large surface area between the receptor subunits (Table 1) and forming a tight three-way junction comprising IL-2Rβ, γ_c, and IL-2. Consistent with the lowest K_d value measured for a single step in IL-2R assembly (28), association of γ_c with IL-2/IL-2β constitutes the ultimate thermodynamic driving force toward the assembly of the IL-2 signaling complex. On activated T cells, IL-2/IL-2β would be part of the ternary IL-2/IL-2Rα/IL-2β complex whereas, on
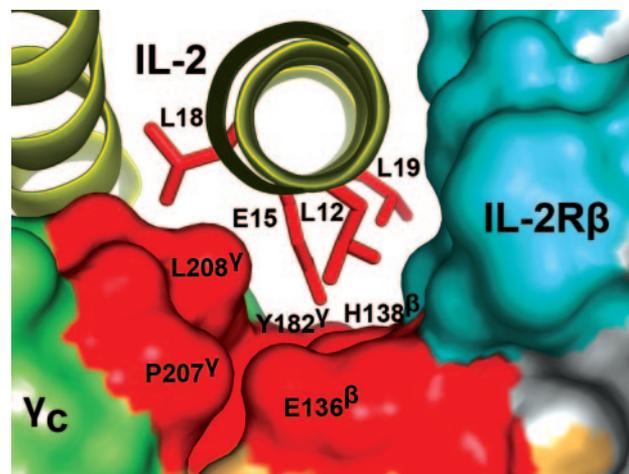

Fig. 5. Three-way junction between IL-2, IL-2Rβ, and γ_c. IL-2 (yellow ribbon representation), IL-2Rβ, and γ_c (the surfaces are colored as in Figs. 3 and 4) form a three-way junction at the heart of the high-affinity IL-2 signaling complex. The network of residues that mediate these contacts (colored red) provides a compelling structural basis for cooperativity in the IL-2/IL-2R complex assembly.

certain natural killer cells and monocytes, IL-2/IL-2β would not be associated with IL-2Rα due to the lack of this receptor subunit on these cells (9). Intriguingly, the buried surface areas of IL-2Rβ and of γ_c that are involved in receptor/receptor and receptor/IL-2 contacts nearly span the entire length of IL-2Rβ and of γ_c. Because the buried surface areas of IL-2Rβ and of γ_c that are involved in receptor/receptor and receptor/IL-2 contacts overlap somewhat (Figs. 3 and 4), we propose that IL-2 binding to IL-2Rβ may induce conformational changes in the contiguous γ_c contact area of IL-2Rβ, which primes the IL-2/IL-2Rα/IL-2Rβ and the IL-2/IL-2Rβ complex, respectively, for γ_c recruitment. The IL-2-dependent IL-2Rβ/γ_c association is further enhanced by three γ_c residues (Tyr-182$^\gamma$, Pro-207$^\gamma$, and L208$^\gamma$), which interface with both IL-2 and IL-2Rβ, two IL-2Rβ residues (Glu-136$^\beta$ and His-138$^\beta$) which are correspondingly buried in IL-2/γ_c interface, and by three IL-2 residues (Leu^{IL12}, Glu-15^{IL2}, and Leu-19^{IL2}), which interface with both receptor subunits (Fig. 5). This cooperative mechanism could then account for the nondetectable affinities (<50 μM) of IL-2Rβ to γ_c in the absence of IL-2, and IL-2 to γ_c (28), and would also provide an essential safety mechanism against premature signaling via the IL-2Rβ/γ_c dimer in the absence of ligand. Collectively, the three-way junction between IL-2, IL-2Rβ, and γ_c provides a compelling structural basis for cooperativity in IL-2/IL-2R complex assembly initiated by, and therefore dependent on, IL-2 or IL-2/IL-2Rα.

The structural features of the IL-2/γ_c interface provide a plausible mechanism of how the common γ chain γ_c is capable of binding to six different cytokines (34). First, the IL-2/γ_c interface is characterized by the smallest buried surface area, and only a portion of the D1/D2 junction of γ_c actually contacts IL-2 (Fig. 4). Second, the relatively large elbow angle between D1 and D2 of γ_c with respect to other cytokine class I receptors increases the prospective ligand-binding surface in the interdomain region. Most strikingly, little specificity is conferred upon the IL-2/γ_c interface due to the formation of only 2 hydrogen bonds, as opposed to 7 and 10 in the other two IL-2/IL-2R interfaces. Our structural results also agree well with extensive mutagenesis work on defining the epitopes on γ_c for various cytokines (25, 26, 35). Tyr-103$^\gamma$, Cys-160$^\gamma$, and Cys-209$^\gamma$, identified as hot-spot residues in all of the cytokine/γ_c interfaces, form a hydrophobic patch in the center of the IL-2/γ_c interface. Because certain residues located around this hot spot were

exclusively implicated in IL-4 binding (Ile-100$^\gamma$ and Leu-102$^\gamma$) or IL-21 binding (Asn-44$^\gamma$, Leu-161$^\gamma$, Glu-162$^\gamma$), a general model for degenerate cytokine recognition by γ_c was proposed in which the various binding sites were largely overlapping, but not identical (26, 35). The lack of effect on cytokine binding of mutations involving Lys-97$^\gamma$, Phe-156$^\gamma$, Leu-157$^\gamma$, Asn-159$^\gamma$, or His-184$^\gamma$ also revealed that this portion of the interdomain region, which in the x-ray structure does not contact IL-2 but IL-2Rα of an adjacent complex in the crystal (see *Results*), does not seem to be involved in binding to other cytokines. Given the relatively small nature and the low specificity of the IL-2/γ_c interface that must largely overlap with other cytokine/γ_c interfaces, the γ_c specificity in the IL-2R complex must then arise from specific interactions of γ_c with IL-2Rβ. Whether the combination of a relatively specific receptor/receptor interaction, but relatively nonspecific receptor/cytokine interaction, also holds for other signaling complexes involving γ_c remains an essential, but unanswered, question. In summary, the composite γ_c-binding site on the binary (IL-2/IL-2Rβ) or tertiary (IL-2/IL-2Rα/IL-2Rβ) complex serves both cooperativity and specificity purposes in the assembly of the high-affinity IL-2 signaling complex.

Upon activation, the high-affinity receptor undergoes rapid endocytosis and subsequent dissociation in the endosome (36). The prevalence of strong electrostatic interactions within the IL-2/IL-2Rα interface (Fig. 2) also provides an excellent structural solution for promoting the dissociation of IL-2Rα from the quaternary IL-2 signaling complex at the lower pH within endosomes. IL-2Rα can recycle back to the plasma membrane whereas IL-2, IL-2Rβ, and γ_c undergo degradation. It is noteworthy that the x-ray structures presented here as well as elsewhere (17) were both determined at acidic pH (5.1 and 6.1, respectively). The determined assemblies may, therefore, be more representative of the structure as it occurs in the endosome, where it is poised for IL-2Rα disengagement. Engineered IL-2 mutants with significantly increased affinity for IL-2Rα increase the potency and persistence of IL-2, possibly by preventing dissociation of IL-2 from IL-2Rα in the endosome and

causing an IL-2/IL-2Rα complex to be recycled to the cell surface (37). This mechanism could account for the differential signaling responses for IL-2 versus IL-15, despite their shared receptor (IL-2Rβ/γ_c), because each ligand binds a unique α chain with very different affinities [$K_d \approx 10$ nM and $K_d \approx 10$ pM (membrane-bound), respectively] (38), and each receptor complex exhibits a distinct pattern of persistence on the cell surface (39), further supporting the role of IL-2Rα as a regulatory ligand carrier.

In conclusion, the crystal structure of the human IL-2 signaling complex has given us the opportunity to address key residual issues on IL-2R assembly, the specific role of the IL-2Rα chain in modulating the signaling response, and the ability of γ_c to act as a component of a variety of additional receptors, as well as to suggest lateral assembly of receptor complexes on the cell surface that could enhance signal propagation.

Materials and Methods

For details on expression, purification, complex formation, crystallization, and structure determination, see *Supporting Materials and Methods*. In brief, the ectodomains of the human IL-2 receptor chains IL-2Rα, IL-2Rβ, and γ_c were individually cloned and expressed in insect cells. Recombinant human IL-2 was kindly provided by Amgen as a gift to K.A.S. The high-affinity IL-2 receptor ligand complex was reconstituted from the individual protein chains by incubation at 37°C and purified by gel filtration. The IL-2/IL-2R complex crystallized in triclinic space group P1. The crystal structure was determined to 3.0 Å resolution by molecular replacement by using the coordinates from an independently assembled IL-2/IL-2R complex (17). Data processing and final refinement statistics are shown in Table 2.

1. Morgan, D. A., Ruscetti, F. W. & Gallo, R. (1976) *Science* **193,** 1007–1008.
2. Robb, R. J. & Smith, K. A. (1981) *Mol. Immunol.* **18,** 1087–1094.
3. Smith, K. A., Favata, M. F. & Oroszlan, S. (1983) *J. Immunol.* **131,** 1808–1815.
4. Taniguchi, T., Matsui, H., Fujita, T., Takaoka, C., Kashima, N., Yoshimoto, R. & Hamuro, J. (1983) *Nature* **302,** 305–310.
5. Baker, P. E., Gillis, S. & Smith, K. A. (1979) *J. Exp. Med.* **149,** 273–278.
6. Smith, K. A. (1988) *Science* **240,** 1169–1176.
7. Klebb, G., Autenrieth, I. B., Haber, H., Gillert, E., Sadlack, B., Smith, K. A. & Horak, I. (1996) *Clin. Immunol. Immunopathol.* **81,** 282–286.
8. Robb, R. J., Munck, A. & Smith, K. A. (1981) *J. Exp. Med.* **154,** 1455–1474.
9. Wang, H. M. & Smith, K. A. (1987) *J. Exp. Med.* **166,** 1055–1069.
10. Leonard, W. J., Depper, J. M., Uchiyama, T., Smith, K. A., Waldmann, T. A. & Greene, W. C. (1982) *Nature* **300,** 267–269.
11. Sharon, M., Klausner, R. D., Cullen, B. R., Chizzonite, R. & Leonard, W. J. (1986) *Science* **234,** 859–863.
12. Teshigawara, K., Wang, H. M., Kato, K. & Smith, K. A. (1987) *J. Exp. Med.* **165,** 223–238.
13. Takeshita, T., Asao, H., Ohtani, K., Ishii, N., Kumaki, S., Tanaka, N., Munakata, H., Nakamura, M. & Sugamura, K. (1992) *Science* **257,** 379–382.
14. He, Y. W. & Malek, T. R. (1998) *Crit. Rev. Immunol.* **18,** 503–524.
15. Smith, K. A. (1995) *Ann. N.Y. Acad. Sci.* **766,** 263–271.
16. Smith, K. A. (2004) *Med. Immunol.* **3,** 3–22.
17. Wang, X., Rickert, M. & Garcia, K. C. (2005) *Science* **310,** 1159–1163.
18. de Vos, A. M., Ultsch, M. & Kossiakoff, A. A. (1992) *Science* **255,** 306–312.
19. Rickert, M., Wang, X., Boulanger, M. J., Goriatcheva, N. & Garcia, K. C. (2005) *Science* **308,** 1477–1480.
20. Sugamura, K., Asao, H., Kondo, M., Tanaka, N., Ishii, N., Ohbo, K., Nakamura, M. & Takeshita, T. (1996) *Annu. Rev. Immunol.* **14,** 179–205.
21. Bork, P., Holm, L. & Sander, C. (1994) *J. Mol. Biol.* **242,** 309–320.
22. Livnah, O., Stura, E. A., Johnson, D. L., Middleton, S. A., Mulcahy, L. S., Wrighton, N. C., Dower, W. J., Jolliffe, L. K. & Wilson, I. A. (1996) *Science* **273,** 464–471.
23. Walter, M. R. (2004) *Adv. Protein Chem.* **68,** 171–223.
24. Syed, R. S., Reid, S. W., Li, C., Cheetham, J. C., Aoki, K. H., Liu, B., Zhan, H., Osslund, T. D., Chirino, A. J., Zhang, J., et al. (1998) *Nature* **395,** 511–516.
25. Olosz, F. & Malek, T. R. (2000) *J. Biol. Chem.* **275,** 30100–30105.
26. Zhang, J. L., Buehner, M. & Sebald, W. (2002) *Eur. J. Biochem.* **269,** 1490–1499.
27. Buchli, P. & Ciardelli, T. (1993) *Arch. Biochem. Biophys.* **307,** 411–415.
28. Rickert, M., Boulanger, M. J., Goriatcheva, N. & Garcia, K. C. (2004) *J. Mol. Biol.* **339,** 1115–1128.
29. Bazan, J. F. (1989) *Biochem. Biophys. Res. Commun.* **164,** 788–795.
30. Holm, L. & Sander, C. (1993) *J. Mol. Biol.* **233,** 123–138.
31. Wu, Z., Goldstein, B., Laue, T. M., Liparoto, S. F., Nemeth, M. J. & Ciardelli, T. L. (1999) *Protein Sci.* **8,** 482–489.
32. Forsten, K. E. & Lauffenburger, D. A. (1994) *Mol. Immunol.* **31,** 739–751.
33. Selzer, T., Albeck, S. & Schreiber, G. (2000) *Nat. Struct. Biol.* **7,** 537–541.
34. Sugamura, K., Asao, H., Kondo, M., Tanaka, N., Ishii, N., Nakamura, M. & Takeshita, T. (1995) *Adv. Immunol.* **59,** 225–277.
35. Zhang, J. L., Foster, D. & Sebald, W. (2003) *Biochem. Biophys. Res. Commun.* **300,** 291–296.
36. Gesbert, F., Sauvonnet, N. & Dautry-Varsat, A. (2004) *Curr. Top. Microbiol. Immunol.* **286,** 119–148.
37. Rao, B. M., Driver, I., Lauffenburger, D. A. & Wittrup, K. D. (2005) *Biochemistry* **44,** 10696–10701.
38. Fehniger, T. A. & Caligiuri, M. A. (2001) *Blood* **97,** 14–32.
39. Dubois, S., Mariner, J., Waldmann, T. A. & Tagaya, Y. (2002) *Immunity* **17,** 537–547.
40. Voss, S. D., Leary, T. P., Sondel, P. M. & Robb, R. J. (1993) *Proc. Natl. Acad. Sci. USA* **90,** 2428–2432.

IMMUNOLOGY